Environ Earth Sci (2015) 73:449–465
DOI 10.1007/s12665-014-3547-4

ORIGINAL ARTICLE

Carbon dioxide, water and energy fluxes of irrigated broad-acre crops in an Australian semi-arid climate zone

Camilla Vote · Andrew Hall · Philip Charlton

Received: 20 December 2013 / Accepted: 12 July 2014 / Published online: 1 August 2014

Abstract The response of the carbon and hydrological cycles of irrigated agro-ecosystems in semi-arid regions to changes in temperature and increasing levels of atmospheric carbon dioxide concentrations is unclear. Furthermore, the extent to which these systems contribute to the carbon cycle as net sources or sinks of carbon dioxide remains relatively unknown. In this study, eddy covariance methodologies were employed to quantify mass and energy exchange of maize, rice and wheat grown in an Australian semi-arid irrigation-dependent agricultural region. It was found that there was a distinct seasonal difference in the magnitude of energy balance components. The latent heat exchange observed during the summer growing season was almost twice that observed during winter. Irrigation management practices significantly influenced the distribution of turbulent fluxes. Over the permanently flooded rice crop, the energy balance was predominately driven by latent heat flux, which accounted for ~99 % of the energy balance. For the crops irrigated intermittently (i.e. maize and wheat), latent heat flux represented ~80 % of the energy balance. In addition, all three crops acted as a net carbon sink over the growing season. The rate of carbon assimilation was impacted by the nature of the photosynthetic pathway of the plant and seasonality. Maize, a C4 plant, exhibited the greatest capacity for carbon uptake ($-1{,}327$ g C/m^2) during the summer months, and winter wheat, a C3 plant, exhibited the least (-388 g C/m^2).

Keywords Eddy covariance · Maize · Rice · Wheat · Australia · Irrigation · Water · Carbon

C. Vote (✉) · A. Hall
School of Environmental Sciences, Charles Sturt University, Locked Bag 588, Wagga Wagga, NSW 2678, Australia
e-mail: cvote@csu.edu.au

A. Hall
Institute for Land, Water and Society, Charles Sturt University, PO Box 789, Albury, NSW 2640, Australia

P. Charlton
School of Computing and Mathematics, Charles Sturt University, Locked Bag 588, Wagga Wagga, NSW 2678, Australia

Introduction

As the global population has increased, the area of global land use dedicated to food production has expanded. For example, during the 18th Century, it is estimated that only 5 % of the Earth's ice-free surface was dedicated to food and fibre production (Spiertz 2012); it is now estimated to be 40 % (Ramankutty et al. 2008). Land use change as a result of population growth, subsequent urbanisation and agricultural intensification has meant that many natural ecosystems have been transformed. Already, most of the suitable, fertile land for agricultural production has been lost (Spiertz 2012) and has not been without cost. For instance, at a continental scale, the annual area of Australian forest conversion to croplands and grasslands in 2009 was 186,383 ha and accounted for 7 % of net greenhouse gas emissions (564.5 million tonnes $CO_{2\text{-e}}$ (Department of Climate Change and Energy Efficiency 2011). Associated land cover changes will affect local surface mass and energy exchange by influencing the way in which radiative fluxes are partitioned at the surface (Foley et al. 2005; Scott et al. 2012). For example, changes to surface albedo and wind field modification properties of the land cover/land use will alter radiative forcing, resulting in surface temperature changes that will affect atmospheric-land surface interactions of water and carbon

dioxide fluxes (Kirschbaum et al. 2013), and thus freshwater availability.

Agricultural activities have been forced to expand into the marginal arid and semi-arid regions of the world (Spiertz 2012); these systems account for 54 % of global food production and produce 45 % of the total global grain yield (Intergovernmental Panel on Climate Change 2007; The World Bank 2007). With a projected population increase of 9 billion people by 2050, it is expected that the pressure on our natural and agro-ecosystems is going to continue to increase. For example, it is predicted that a further 1 billion hectares of natural ecosystems will be lost to provide food and fibre to the future global population (Khan and Hanjra 2009). In addition to the loss of services provided by these ecosystems, the change in land cover and land use at this scale will alter the global mass and energy balance and thus, water and carbon cycles, although to what extent remains relatively unknown (Gilmanov et al. 2010).

In many semi-arid irrigated areas, increased climate variability and agricultural expansion and intensification have already altered the mass and energy balance. This is evidenced by decreased precipitation, reduced runoff and, thus, decreased water availability (Intergovernmental Panel on Climate Change 2007). Although the response of the water and carbon balance of agro-ecosystems to increased climate variability is uncertain (Domingo et al. 2011; Kanniah et al. 2011), it is predicted that further increases to surface temperatures and levels of atmospheric carbon in these areas will have a negative impact on productivity through alterations to crop physiology and decreased yields, particularly those of rice, wheat and maize (Khan and Hanjra 2009; Yu et al. 2012) and future irrigated agricultural production in these areas may be unsustainable.

Furthermore, it is widely acknowledged that the landscape function of various ecosystems of forest, wetlands and tundras are generally found to be carbon sinks (Gilmanov et al. 2010). However, the level of contribution of agricultural broad-acre cropping systems to the carbon cycle as a source or a sink of atmospheric carbon dioxide remains unknown. To adapt to a changing climate, it is necessary to understand the processes of mass and energy exchange and the functions that drive them. Therefore, in-depth and up-to-date information regarding the estimation of water, carbon and energy cycles of irrigated broad-acre crops is required (Kalfas et al. 2011; Yu et al. 2012). This can be achieved through the implementation of Eddy covariance (EC) methodologies which provide the most direct and defensible means of land surface flux estimation (Baldocchi 2003).

In Australia, the interaction between water and carbon dioxide fluxes of irrigated broad-acre crops as measured by EC systems are yet to be reported. Therefore, the results of this study will, for the first time, provide accurate and up-to-date information regarding energy, water vapour and carbon dioxide fluxes of the most commonly irrigated broad-acre crops grown in semi-arid areas of Australia. These irrigated farming systems are of particular importance to the Australian community due to the significant economic value which contributes 31 % of the gross value of agricultural production in the Murray Darling Basin (MDB; Australian Bureau of Statistics 2012a); and account for 54 % of the total national water consumption (Australian Bureau of Statistics 2012c). The objectives of this study are to: quantify and examine the seasonal distribution of energy, water and carbon fluxes of three major crops, i.e. maize, rice and wheat, grown in an Australian irrigation system located in the semi-arid regions of the southern MDB; and to determine whether irrigated agro-ecosystems in Australian semi-arid climate zones are net sources or sinks of carbon dioxide.

General description of the study area

The Coleambally Irrigation Area (CIA) is a gravity-fed irrigation system in the Riverina district of southern New South Wales, Australia (see Fig. 1). This region is one of two major irrigation areas located within the larger Murrumbidgee catchment. In 2010/11, the total gross value of agricultural commodities produced in the Riverina was $1.8 billion, with broad-acre crops accounting for $1.4 billion (Australian Bureau of Statistics 2012b). The CIA, as an agro-ecosystem, contains 79,000 ha of intensively irrigated land. A further 325,000 ha of the surrounding area is serviced with stock, tank and opportunistic irrigation water (Jackson et al. 2010). Summer (November–April) crop production primarily consists of rice and maize, with lesser plantings of soybean, sorghum, cotton, sunflowers and other horticultural/viticultural activities. The production of wheat, barley, canola and pasture constitute the major winter activities (May–October) (Coleambally Irrigation Cooperative Ltd 2011). With a slope of close to 0°, the topography of the area is considered 'pan flat' (McVicar and Van Niel 2012). Common soil types found in the CIA consist predominately of self-mulching clays, red-brown earths and transitional red-brown earths, each well suited to irrigated crop production. Based on temperature and humidity, the climate experienced within the CIA is classified as having hot, dry summers and cold winters (Bureau of Meteorology 2005). The mean maximum January temperature is 32.8 °C and the mean maximum July temperature is 14.5 °C, which is consistent with temperate semi-arid conditions (Bureau of Meteorology 2012). The average precipitation is 406.5 mm/year with no distinct seasonal variability. Long-term average annual potential evapotranspiration rates are 1,861 mm and mean annual global solar radiation is 6,450 MJ/m^2 (Coleambally

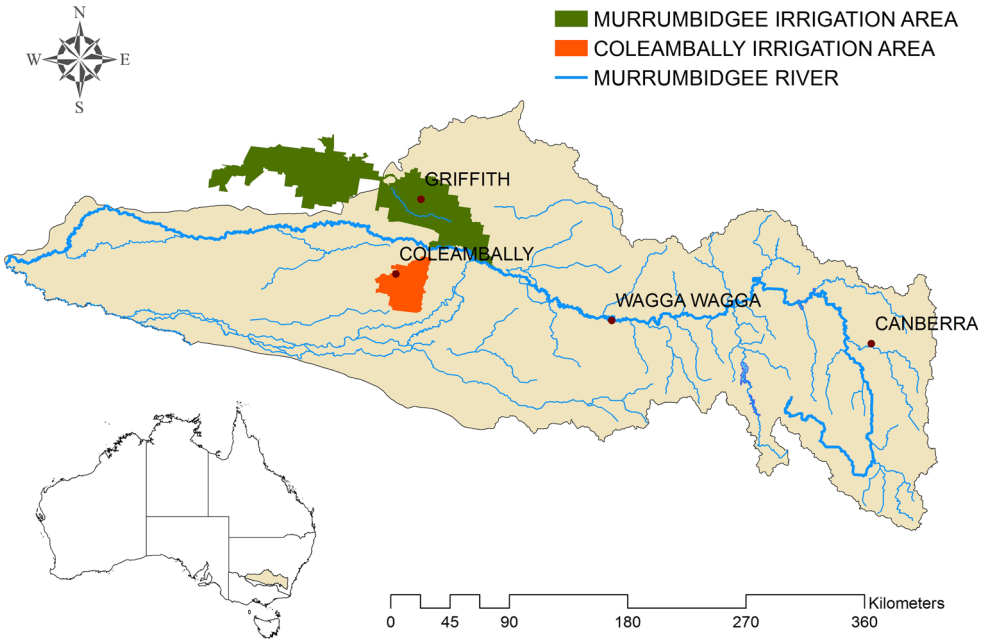

Fig. 1 Murrumbidgee catchment and major irrigation areas

Irrigation Cooperative Ltd 2010; Bureau of Meteorology 2012). Whilst the levels of mean global solar radiation are more than adequate to sustain the intensive agricultural cropping methods common in this region, monthly evapotranspiration exceeds precipitation throughout the year. For these reasons, supplementary irrigation water is required to meet crop water demand, particularly during the summer growing season. The most common source of irrigation water in the CIA is surface water, which accounts for 98.7 % of total irrigation water supplied. In 2010/11, rice was the largest consumer of irrigation water in the CIA and accounted for 65.1 % of irrigation water delivered. Maize and wheat accounted for 6.9 and 4.8 %, respectively. The total areas of rice, maize and wheat plantings were 14,512, 4,367 and 11 334 ha, respectively (Coleambally Irrigation Cooperative Ltd 2011).

Site selection, flux measurement and micrometeorology

Site selection was based on the three major broad-acre crops produced in the area: rice and maize grown over the summer months and wheat, the predominant winter crop. Adequate fetch (or footprint) upwind of sensors was the primary consideration to ensure that mostly all observed fluxes were representative of the single cultivar of interest. A number of factors, including wind speed and direction, canopy height, surface roughness and instrumentation height above the canopy were considered. The willingness of the landowner to participate in the experiment was also an important consideration.

The mass and energy exchanges of the selected cropping systems were measured by employing EC technologies. Through the implementation of fast response sensors, direct measurement of carbon dioxide, water vapour and energy fluxes between the land surface and the atmosphere was achieved. The EC instrumentation for the three installations (hereby referred to as flux towers) was almost identical. Two flux towers were placed in situ over each growing season in 2010/11 to monitor the mass and energy exchange of the two major summer crops cultivated in the area, maize and rice and the major winter crop, wheat. Both flux towers consisted of a three-dimensional sonic anemometer (CSAT3, Campbell Scientific Inc., USA), which measured fluctuations in longitudinal, lateral and horizontal wind speed and direction (u, v, w; m/s), and an open-path infrared gas analyser (LI-7500, LI-COR Inc., USA) designed to measure CO_2, water vapour and momentum fluxes. Both the sonic anemometer and gas analyser were positioned to face into the expected prevailing wind direction on a boom that extended 1 m horizontally from the tower. To monitor water and carbon dioxide flux response to micrometeorological drivers, instantaneous measurements of flux variables were required (Burba 2013), therefore the sampling rate of each system was set at 10 Hz and recorded with a data logger (CR3000, Campbell Scientific, Inc. USA). The fluxes (as a measure of the covariance between the scalar (e.g. CO_2 or H_2O) and the vertical wind component) were then computed as an average of the 10 Hz data over 30 min intervals. Both the 10 Hz data and the 30 min averaged data were recorded on a 2 GB Compact Flash card which was downloaded on a monthly basis.

Micrometeorological instruments were also stationed at each site to complement the EC flux measurements. Ancillary observations of wind speed and direction were made with a standard wind vane and anemometer (RM

Table 1 Flux tower locations and agricultural indices

Crop	Flux tower #	Longitude	Latitude	Sown	Harvested	Crop area (ha)	Yield (t/ha)	Irrigation water applied (ML/ha)
Maize	1	−34.760	146.015	7/10/2010	4/4/2011	60	12.0	5.6
Rice	2	−34.925	145.821	12/11/2010	20/4/2011	100	10.1	7.6
Wheat	1	−34.760	146.015	6/5/2011	3/12/2011	60	5.0	2.6

Young Wind Sentry 3001, Campbell Scientific, Inc. USA). Air temperature and relative humidity were measured with an aspirated and shielded thermistor and capacitance sensor (HMP45C, Campbell Scientific, Inc. USA), and a tipping bucket rain gauge (TB3, Hydrological Services Pty. Ltd. Australia) was used to measure rainfall. Net radiation (R_n) was measured using a four-component net radiometer (CNR1, Kipp & Zonen B.V.) on a boom fixed 2 m above the ground surface and oriented to the north. Ground heat flux (G) was measured using two self-calibrating soil heat flux plates (HFP01SC, Hukseflux Thermal Sensors B.V.) at distances of 10 m to the north and 25 m to the west of each flux tower. These were buried at depths of 80 mm in conjunction with two thermocouple configurations buried 1 m apart at depths of 60 and 20 mm (114 TCAV-L, Campbell Scientific Inc., USA). Volumetric soil moisture content was not measured. In the absence of suitable time series data, a default value based on soil samples taken at each site was used to calculate the heat storage in the soil layer above the heat flux plates. Solar radiation values were taken from a nearby weather station operated and maintained by Coleambally Irrigation Cooperative Limited (CICL). These weather stations were located within distances of 20 km or less of the flux towers. Details of flux tower location, crop area and other agricultural indices are given in Table 1.

Data processing and gap-filling

Cospectral analysis

The application of EC technologies to determine mass and energy balances has not yet been reported within an Australian irrigated agricultural environment. It was necessary, therefore, to perform a comprehensive cospectral analysis to determine an averaging period to ensure all significant low-frequency eddies would be accounted for. This can be achieved through an ogive test, represented by the cumulative integral of the cospectrum, beginning with the highest frequency (Foken et al. 2006). To perform the ogive test, the raw, non-gapfilled 10 Hz data were processed using open-source software, EdiRe©. Day-time data were integrated over 120 min averaging periods between the hours of 07:00 and 19:00 Australian Eastern Standard Time (AEST) for both summer and winter crops to avoid the influence of the daily cycle of fluxes and non-steady state conditions; longer periods are generally not scrutinised due to the daily cycle of fluxes and high non-steady state conditions (Foken et al. 2006). Because the ogive test fails if missing values occur within the time series, intervals devoid of gaps were included in the analysis, avoiding the bias of abnormal cospectra. In this study, ogives were constructed based on sensible heat flux co-spectra ($w'T_{sonic}'$). The main reason for doing so was because the sonic temperature (T_{sonic}) and vertical wind speed (w) were instantaneously derived from the sonic anemometer, negating the need to account for sensor separation or time delays between two signals (i.e. if temperature and wind speed were measured by two different instruments). As such, $w'T_{sonic}'$ was considered close to ideal, and the actual scalar flux (water vapour or CO_2) would lie somewhere below this curve (Burba and Anderson 2010).

Spike detection, corrections and gap-filling

The flux data that were averaged over each 30 min interval was post-processed using standard EC protocols and software developed through the OzFlux community (Isaac and Cleverly 2011), further modified to suit the needs of this study. For instance, additional calculations were incorporated into the programme to account for the heat storage in the water column to calculate storage heat flux (G) for the rice crop (see "Determination of energy balance components"). Detailed information regarding the specific corrections is presented in Table 2. Once all data had been processed, a gap-filling procedure was implemented whereby data gaps of less than 60 min were filled using simple linear interpolation techniques and larger gaps were filled using daily climatologies calculated for the same observation period.

Flux footprint analysis

Due to limited water supplies, crops grown in the CIA are limited in their spatial extent and are often grown alongside non-irrigated fallow lands and remnant vegetation. Given the heterogeneous nature of irrigated farmland in the CIA,

Table 2 Corrections and calculations applied to flux data to produce a non-gap-filled dataset

Correction/calculation	Purpose	Primary references
Two dimensional co-ordinate rotation	To align the mean lateral and vertical velocities to zero i.e. $\overline{u} = \overline{w} = 0$	Lee et al. (2004)
Calculate air temperature (T_a) from virtual temperature (T_v), absolute humidity and pressure	To provide a more robust measurement of air temperature based on sonic thermometry measurements (i.e. as measured by the CSAT3)	Loescher et al. (2005)
Frequency response corrections	This includes a suite of corrections to compensate for flux losses as a result of spectral attenuation (invoked by sensor design and time response, sensor separation, electronic filters etc.)	Massman (2000, 2001); Massman and Clement (2004)
Flux calculation	Calculate fluxes from covariances	Lee et al. (2004)
Webb Pearman Leuning (WPL) corrections	To compensate for fluctuation effects of temperature and water vapour on LE and CO_2 fluxes	Leuning (2004); Webb et al. (1980)
Correct G for storage	To calculate the heat stored in the soil layer above the soil heat flux plate and incorporate this into estimates of G	Campbell Scientific Inc. (2007)
Friction velocity (u^*) threshold	To correct for the underestimation of night-time F_c fluxes (see "Determination of friction velocity threshold")	
Removal of contaminated fluxes from quadrant opposite orientation of EC sensors	Turbulent flux data was also removed to prevent the influence of flow distortion as a result of air passing through the tower and solar powered battery array behind the sensors	Zhang et al. (2013)

it is necessary to ensure that the source emissions are representative of the area of interest. The effective fetch (or flux footprint) was modelled using the Microsoft® Excel based ART (Agroscope Reckenholz-Tänikon) Footprint Tool designed by Neftel et al. (2008).

Surface energy balance

Determination of energy balance components

Based on the first law of thermodynamics, the sum of the sensible heat flux (H_s) and latent heat flux (LE) is equal to the available energy (i.e. the net radiation minus the ground heat flux, $R_n - G$), given by the equation (modified from Brutsaert 1982):

$$R_n - G = H_s + \mathrm{LE}$$

For the rice crop, additional components of G were incorporated to account for the heat storage in the floodwater (W) as well as the soil heat storage (S), adapted from Tsai et al. (2007), i.e.

$$R_n - S - W = H_s + \mathrm{LE}$$

where

$$S = \rho_g c_g z_g \frac{\partial T_g}{\partial t}$$

and

$$W = \rho_w c_w z_w \frac{\partial T_w}{\partial t}$$

where ρ_g and ρ_w represent the density of wet soil and water, respectively; c_g and c_w represent the heat capacity of wet soil and water, respectively; z_g and z_w are the depth of the soil heat flux plates in relation the soil surface and the depth of the floodwater, respectively; and dT_g/dt and dT_w/dt represent the rates of change in soil temperature and water temperature, respectively. In the absence of water temperature data, the average air temperature, as measured by the EC system, was used to estimate W, based on the assumption that mean water temperature is similar to mean air temperatures, after De Datta (1987).

Energy balance closure

An audit of the energy balance is required to assess the overall performance of the EC instruments and to obtain an independent assessment of the scalar flux estimates under any given conditions. When using EC systems, the sum of the estimated turbulent fluxes ($H + LE$) is generally less than the estimated available energy (Leuning et al. 2005). To date, studies have found that the average energy balance closure of various ecosystems range from 0.75 to 0.87 (Stoy et al. 2013). In this study, an evaluation of the energy balance closure was determined specifically by using the Energy Balance Ratio (EBR) of the half-hourly averaged flux estimates over the observation period (Tsai et al. 2007; Wilson et al. 2002). The EBR is given by the equation:

$$\mathrm{EBR} = \frac{\sum(H + \mathrm{LE})}{\sum(R_n - G)}$$

Evapotranspiration

Actual evapotranspiration (ET_a) is represented by LE and is directly measured by the EC system (see "Determination

of energy balance components"). To compare how these values perform against traditional methods of evapotranspiration estimation, reference crop evapotranspiration (ET_o) and potential crop evapotranspiration (ET_c) were calculated using the established methods described by Allen et al. (1988). Crop coefficients defined by (Meyer et al. 1999) that were used to determine ET_c in the Murrumbidgee Irrigation Area (see Fig. 1) were also used to estimate ET_c in the CIA, given its proximity to the study area.

Carbon fluxes

Determination of friction velocity threshold

The friction velocity (or u^*) threshold is used to determine stable atmospheric conditions and can be used to correct for the underestimation of night-time CO_2 fluxes and determine ecosystem components of carbon metabolism (GPP, NEE and Re). The u^* threshold can be found by plotting night-time values of u^* against corresponding CO_2 fluxes; the u^* threshold is located at the point where the fluxes begin to decrease as u^* decreases (Jans et al. 2010). To determine the u^* threshold, rank-ordered night-time u^* values and corresponding CO_2 fluxes were divided into 25 groups. The average values of each group were then calculated and plotted to evaluate the relationship between u^* and CO_2 flux (Long 2008).

Partitioning of carbon dioxide fluxes to determine gross primary productivity and total ecosystem respiration

EC systems can provide direct measurements of net ecosystem exchange (NEE, measured as CO_2 fluxes), but they cannot directly measure gross primary productivity (GPP) or total ecosystem respiration (Re). Instead, models are required to partition NEE into GPP and Re (Baldocchi et al. 2001) where NEE, as defined by Falge et al. (2002) and Wohlfahrt et al. (2005) is given by:

$$\mathrm{NEE} = \mathrm{Re} - \mathrm{GPP}$$

Based on the assumption that GPP is equal to zero at night (as there is no photosynthetic activity), total Re is equal to NEE. The difference between day-time NEE and night-time NEE can be used to calculate GPP using an empirical model to extrapolate nocturnal respiration (Goulden et al. 2011). As Re is sensitive to temperature (Lloyd and Taylor 1994), night-time CO_2 fluxes were plotted against corresponding soil temperatures, and a simple exponential function was fitted to the data (Leuning et al. 2005). This equation is given by:

$$\mathrm{Re} = A \exp(\mathrm{BT})$$

where A and B are empirical constants determined by regression and T is temperature. This exponential function was then used to deduce day-time estimates of Re. GPP was then estimated as the difference between day-time Re and NEE (Evrendilek et al. 2011; Falge et al. 2001; Reichstein et al. 2005). The application of this methodology also enables the correction of night-time carbon dioxide fluxes that may be underestimated due to periods of atmospheric stability (as indentified by the u^* threshold) by adjusting fluxes according to the same exponential function [as night-time CO_2 flux (NEE)] is equal to night-time Re.

Results and discussion

Climatic conditions

The long-term averages of rainfall and temperature experienced in the CIA (1958–2012) are presented in Fig. 2. The mean air temperatures and rainfall observed at each flux tower location are also presented here. The total annual rainfall received in the CIA in 2010/11 was the highest on record. The majority of this rain was observed during the summer growing season where the total rainfall from November–April was 476 mm. The observed winter rainfall (May–October) was 204 mm. The observed mean maximum air temperature over the summer and winter growing season was 29.4 and 18.2 °C, respectively.

Cospectral analysis

The ogives constructed for each crop during the vegetative growth stage are presented in Fig. 3. All significant low-frequency eddies were captured within a 10–30 min period for all three cropping systems as illustrated by the ogive curves reaching an asymptote within this timeframe (Moncrieff et al. 2004). Therefore, the 30 min averaging period, consistent with standard processing methods of the wider flux community was selected for further processing and analysis in this study.

Spike detection corrections and gap-filling

Table 3 illustrates the percentage of flux data removed and subsequently gap-filled for each experimental site in this study. The average percentage of CO_2 flux data that was removed from all three time series datasets was 47.8 % with a range of 45.7–50.7 %. The average amount of LE data removed was 36.6 % and the range was 32.7–39.9 %. During the day, the quality control flags indicated that the majority of the data was removed as a result of gas analyser and sonic anemometer failure. These gaps generally coincided with rainfall events, which are known to affect the operation and accuracy of EC sensors (Burba and Anderson 2010). Given the atypical amount of rainfall received in the

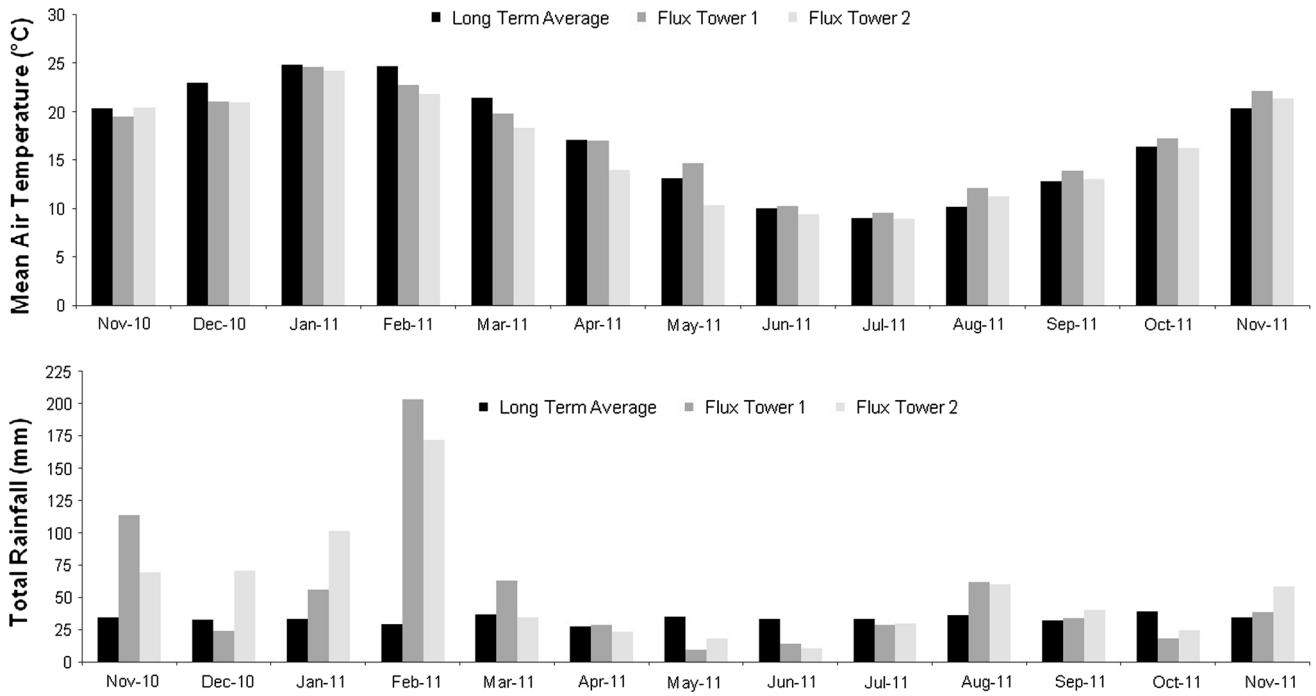

Fig. 2 Total monthly rainfall and average monthly air temperatures observed at both flux tower locations for the period Nov 2010–2011. The long-term averages are also given (Bureau of Meteorology 2012)

CIA in 2010/11, a larger amount of CO_2 and LE flux data than was originally anticipated required gap-filling. Additional gaps in CO_2 flux data were the result of a large number of night-time fluxes that registered below the u^* threshold and were subsequently corrected (see "Partitioning of carbon dioxide fluxes to determine gross primary productivity and total ecosystem respiration").

The percentage of H_s gap-filled data was similar for all flux tower sites (4.0 and 3.9 %) with the exception of the wheat crop (19.1 %). This can partially be attributed to instrument failure during the first week of the observation period at the wheat site. Whilst the amount of gap-filling required for each dataset was typical of EC studies where gaps are generally found to account for 20–60 % of an annual dataset (Moffat et al. 2007), their existence is a cause for concern. A significant proportion of the turbulent flux data has been interpolated; therefore the results reported in this study may be heavily influenced by random and systematic bias error.

Flux footprint analysis

Figure 4 depicts the location of the flux tower and the 90 % cumulative probability of the source emissions in relation to the boundaries of the experimental sites. As demonstrated, the effective fetch during the night at each experimental site was greater than what it was during the day. This can be attributed to the greater proportion of low wind speeds and more stable atmospheric conditions that generally occur at night (Burba and Anderson 2010). For both summer crops, the effective fetch was representative of the field of interest (i.e. within the boundaries of the paddock) for day-time and night-time conditions. During the winter, the night-time flux footprint over the wheat crop extended beyond the field boundaries. In this instance, fluxes may have been influenced by the presence of Eucalypt trees that lined the north-eastern boundary as well as the adjacent block of fallow land, directly east of the crop. However, at night, the majority of the winds (approximately 73 %) originated between compass bearings of 90°–360°. Additionally, all fluxes originating from a bearing of 45°–135° were filtered from the time series as part of the quality control process. Therefore the cumulative flux contribution that originated from the north east to south east at distances greater than 187 m (the shortest distance to the boundary) was considered negligible.

Energy balance

The mean EBR of maize, rice and wheat was 0.80, 0.71 and 0.65, respectively, typical of EC studies of agricultural crops conducted elsewhere. For example, Stoy et al. (2013) conducted a synthesis of 173 sites of various plant functional types (including forests, wetlands, savannas and agricultural crops) that showed that the mean energy balance closure was 0.84 with a range of 0.28–1.67. Stoy et al. (2013) also showed that agricultural cropping systems were among the worst performers (mean EBR = 0.78),

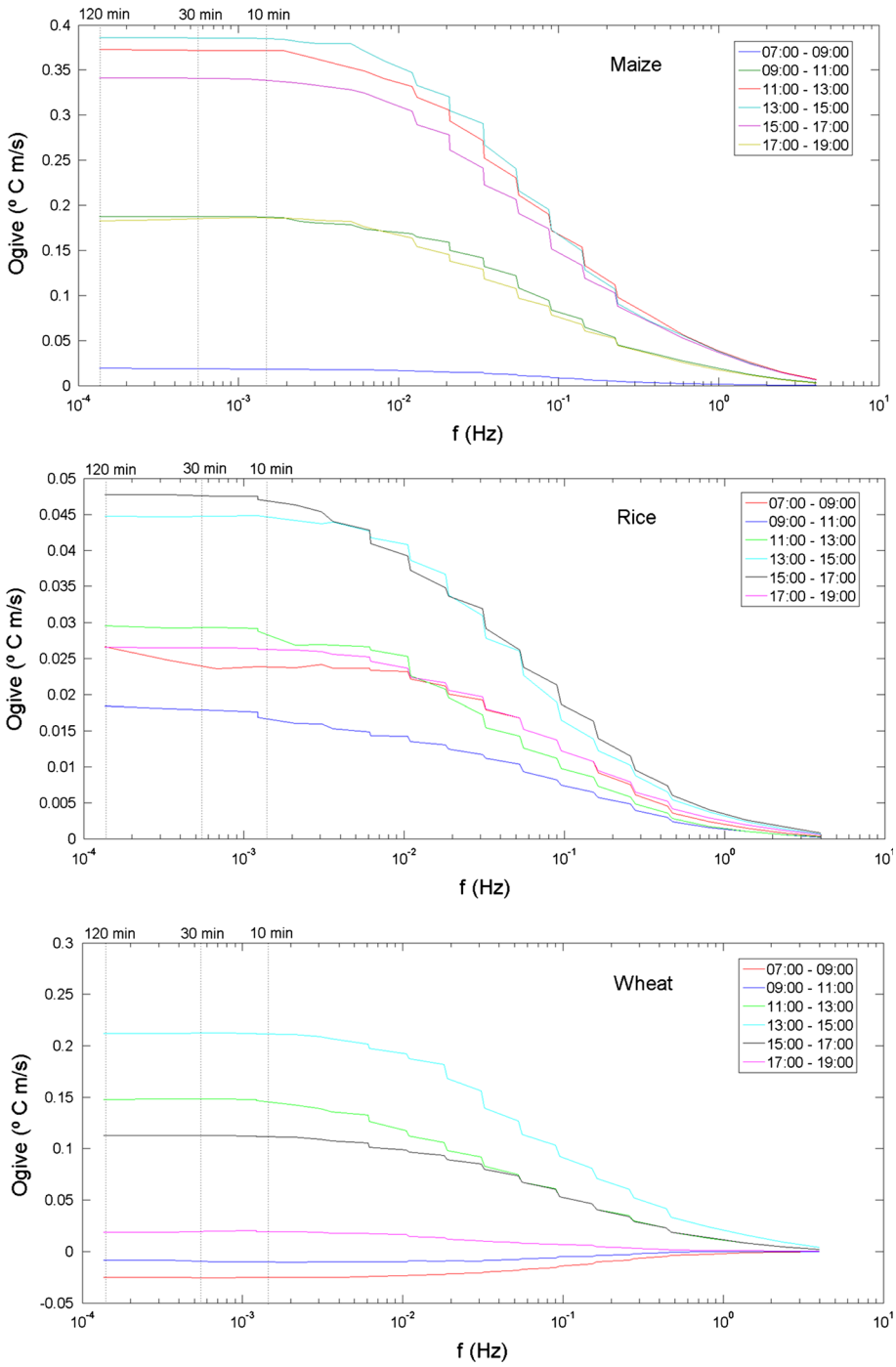

Fig. 3 Ogives (°C m/s) for maize, rice and wheat during the vegetative stage

Table 3 Percentage (%) of flux data that required gap-filling

Crop	F_c	LE	H_s	R_n	G
Maize	46.9	32.7	4.0	0.4	0.1
Rice	50.7	37.1	3.9	4.9	25.5
Wheat	45.7	39.9	19.1	4.2	4.7

alongside wetlands and mixed forests. The lack of energy balance closure can be partially attributed to the underestimation of the turbulent heat fluxes. This generally occurs as a result of the failure to include one or more of the storage flux components in the air column beneath the EC instrumentation. This includes not only soil heat storage, but also heat storage within the plant biomass, heat storage

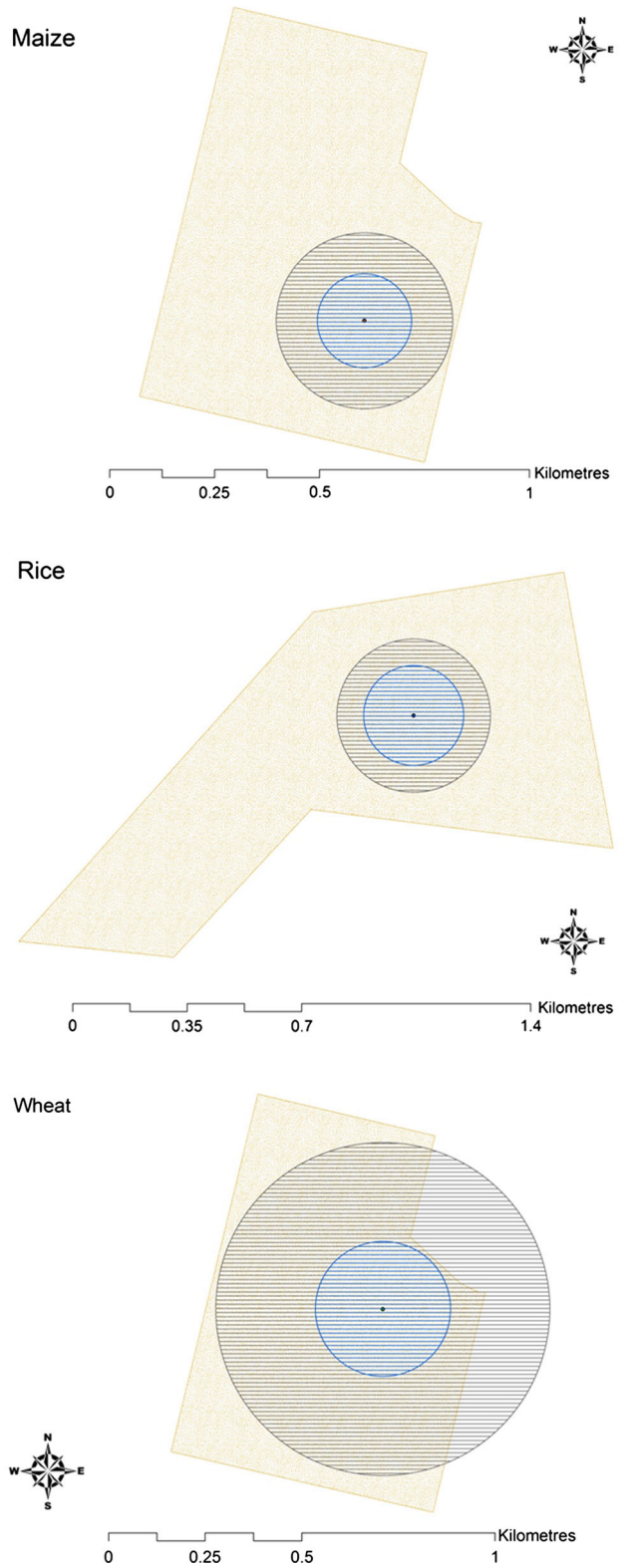

Fig. 4 Flux footprint of the maize, rice and wheat crop. Note that the *blue circle* represents the effective fetch during the day; the *grey circle* represents the effective fetch at night

within the canopy air mass and biochemical photosynthetic energy consumption (Kilinc et al. 2012). To incorporate these components would require the observation of additional meteorological and biometric parameters, which, due to resource limitations, were unable to be measured during this study.

Further underestimation of storage heat flux (G) may also be attributed to the failure to measure volumetric soil water content at each flux tower location, which is required to calculate the specific heat capacity of soil to accurately determine soil heat storage (Oncley et al. 2007). In this study, a default value based on soil samples taken at each site was used to calculate G. Therefore, the variation in soil moisture and thus G, as a result of precipitation and irrigation events was unaccounted for. The energy balance observed over the rice crop was further impacted by the need to account for an additional component of G, i.e. the energy stored in the water column (W) required for rice production in the CIA (see "Determination of energy balance components") which also requires additional observations of temperatures in the water column, which were not measured in this study. Instead, the average air temperature measured above the canopy by the EC system was used to calculate W based on the assumption that day-time water temperature fluctuation is minimal and that mean water temperature is similar to mean air temperatures, after De Datta (1987). This approximation of temperatures in the water column may have led to an overestimation of G, increasing the energy imbalance at this site. Furthermore, dynamic and thermal heterogeneities between land surfaces can modify the air flow in the atmospheric boundary layer (Inagaki et al. 2006). Thermal heterogeneities, in particular, have a strong impact on the flow structure that can lead to in-homogenous surface heating, creating a horizontal pressure gradient that can then generate eddies at greater timescales (mesoscale circulations) that are not measured by the EC system (Foken et al. 2010; Inagaki et al. 2006). Therefore the difference between the surface roughness and spectral properties between two neighbouring fields (fallow or otherwise) would distort air flow in the atmospheric boundary layer, further impacting the energy balance.

Seasonal distribution of energy balance components

The cumulative totals of the energy balance components observed at each flux tower location are presented in Table 4. There is a distinct seasonal distribution of energy balance components between the summer and winter crops. The magnitude of latent heat exchange observed during the

summer growing season was almost 50–100 % greater than that of the latent heat exchange observed during winter. For example, the cumulative total of LE for the summer rice and maize crop was 1,920 and 1,530 MJ/m^2, respectively; LE of the winter wheat crop was only 954 MJ/m^2.

The partitioning of available energy (R_n–G) into sensible (H_s) and latent heat (LE) fluxes was also very similar for the summer maize and winter wheat crop where H_s accounted for 19.9 and 18.7 % of the total heat fluxes (H_s + LE), respectively. The rice crop displayed very different behaviour, where H_s accounted for less than 1 % of total heat flux, indicating that the energy balance was predominately driven by latent heat exchange, consistent with the findings of previous studies of energy exchanges of rice (e.g. Hatala et al. 2012; Alberto et al. 2009, 2011). The difference in energy partitioning is most likely the direct result of the different water management strategies adopted for each crop. For example, for the maize crop, a total of 5.6 ML/ha of irrigation water was supplied intermittently throughout the growing season; for the rice crop, a permanent application of water (7.6 ML/ha) was required to maintain levels of 0.05–0.3 m above the soil surface throughout the majority of the growing season (see Table 1). The presence of the permanent water led to greater rates of evaporation from the surface and hence, latent heat exchange. This is particularly relevant during the early vegetative growth stages when the water surface was directly exposed to atmosphere. H_s is further suppressed by the dense rice plant canopy during the warmest period of the growing season (Hatala et al. 2012). For the rice crop, this occurred during the reproductive growth stage, especially between December 23, 2010 and January 29, 2011 (data not shown). During this particular interval, the average air temperature was 29.4 °C and H_s had an average of −1.6 MJ/m^2/day and a range of −5.0 to 1.4 MJ/m^2/day. In contrast, the average air temperature during the entire vegetative stage was 27.0 °C, and H_s averaged 0.4 MJ/m^2/day with a range of −5.0 to 3.5 MJ/m^2/day.

The contribution of G to total available energy was small and ranged between ~1.0 and 2.0 % for maize and wheat with the exception of the rice crop where G accounted for 8.8 % of the available energy. Maximum daily average values of G observed at the maize and wheat sites did not exceed 2.6 MJ/m^2. This indicated there was significant shading beneath the canopy that did not allow for direct heating of the soil (Kilinc et al. 2012). For the rice crop, the maximum rate of G observed was 12.6 MJ/m^2. This is directly related to the additional components of G that must be incorporated to account for the heat storage in the permanent irrigation water application (W) as well as the soil heat storage (S). Despite similarities in magnitude of contribution, the nature of G was very different between the seasons. During the summer months, the cumulative total of G was positive, indicating heat was being absorbed by the surface. During winter, the cumulative total of G was negative, an indication that heat was being lost from the surface.

Table 4 Seasonal distribution of energy balance components (MJ/m^2)

Crop	No. of days of observation	R_n	G	H_s	LE
Maize	158	2,566	21	504	1,530
Rice	160	2,931	259	−19	1,920
Wheat	211	2,035	−34	388	954

Evapotranspiration

Table 5 presents the cumulative totals of ET_o, ET_c and ET_a observed at each of the flux tower locations during the observation period. As mentioned in the previous section, the cumulative totals of ET_a (i.e. latent heat flux) during the summer growing season were ~1.5–2.0 times greater than those of the winter growing season. During the summer months, atmospheric demand is generally greater due to increased temperatures and higher levels of incoming radiation, thus increasing rates of evaporation from soil surfaces and plant material. Differences in water management practices affect the partitioning of energy fluxes, and, consequently, ET_a, and is evident in the differences in the ET_a observed in the two summer crops. For instance, rice had a seasonal ET_a budget that exceeded that of maize by 25 %. The ongoing presence of water for the rice crops led to an average ET_a rate of 4.9 mm/day, whereas the average rate of ET_a for the maize crop was 3.9 mm/day. The average rate of ET_a of wheat was 1.8 mm/day. It is important to note that the average daily rates of ET_a, particularly for the rice crop, are atypical of those usually observed in the CIA. For example, Evans (1971) found that average daily rates of evapotranspiration of rice grown in the region ranged between 1.8 and 14 mm/day. In this study, daily rates of ET_a of the rice crop ranged between ~0.5 and 8.0 mm/day. Atypical rates of ET_a can be partially attributed to the unusually high precipitation.

Humphreys et al. (1994) also found that rice water use (i.e. irrigation + rainfall − deep percolation − surface drainage) varied between 9.0 and 15.4 ML/ha, depending

Table 5 Cumulative totals of reference evapotranspiration (ET_o), potential crop evapotranspiration (ET_c) and actual evapotranspiration (ET_a) observed at each site (mm)

Crop	No. of days of observation	ET_o	ET_c	ET_a
Maize	158	716	490	624
Rice	160	808	834	783
Wheat	211	771	575	389

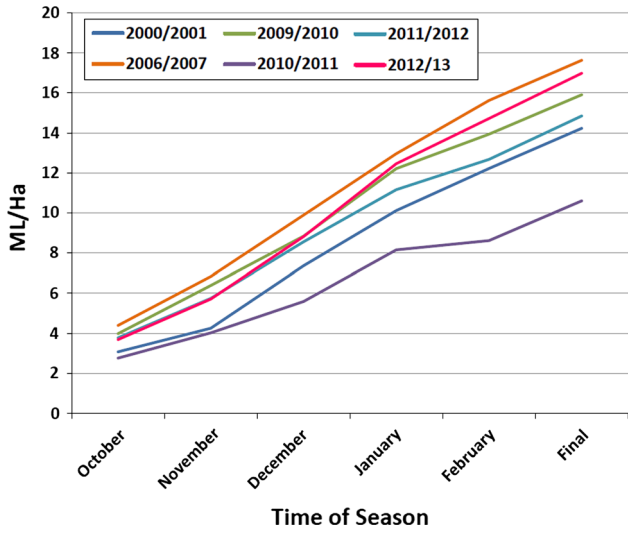

Fig. 5 Seasonal comparison of rice water use (ML/ha) in the Murrumbidgee Irrigation Area (Murrumbidgee Irrigation Ltd 2013)

on the climatic conditions experienced during the growing season. Figure 5 also illustrates the annual average rice water use in the Murrumbidgee Irrigation Area, which, given its proximity to the study area (see Fig. 1), experiences a similar climate to the CIA. As depicted, total rice water use was lowest in 2010/11 (approximately 10.7 ML/ha) and greatest in 2006/07 (approximately 17.8 ML/ha). Generally, for rice production in the CIA, 2 ML/ha of irrigation water is required to fill the soil profile; surface drainage accounts for an additional 2 ML/ha (Smith D, personal communication, March 25, 2013). In this particular study, total input was 7.6 ML/ha (irrigation) + 4.7 ML/ha (rainfall) = 12.3 ML/ha. Subtracting deep percolation and drainage losses, total rice water use was 8.3 ML/ha. The results of the study showed that the cumulative total of ET_a for the rice crop was 783 mm (or ~7.8 ML/ha). According to these figures, there is a remaining 0.5 ML/ha unaccounted for (8.3 − 7.8 = 0.5 ML/ha). Given that 2010/11 marked the end of a 10-year drought in the region, this additional water was most probably lost through deep percolation required to fill very dry soil profiles (Smith D, personal communication, March 25, 2013).

Previously published values of monthly ET_o and ET_c of maize were also greater than those estimated in the CIA in 2010/11 (see Table 6). Except for November, the monthly evaporative demand of the atmosphere (represented by ET_o) reported by Edraki et al. (2003) was ~10–20 % greater than what it was in 2010/11. Additionally, crop water use (represented by ET_c) in 1998/99 was almost double that of crop water use in 2010/11. The total observed rainfall in 2010/11 was much greater than in 1998/99, particularly during the months of November and February.

Whilst evapotranspiration values of the two summer crops grown in the CIA in 2010/11 were consistently higher than previously reported values, it is difficult to say whether or not the values of evapotranspiration of wheat observed in the CIA in 2011 were typical of wheat grown in the area in other years. Table 7 presents the monthly ET_o and ET_c values of wheat grown in 1999 (Edraki et al. 2003) and 2011 (this study). As illustrated, monthly ET_o and ET_c values of wheat grown in 2011 were greater than those reported for 1999 in the first few months of the growing season (June–September), and less in the latter part of the season.

Cumulative ET_c rates of the summer maize crop underestimated ET_a by ~11 %. This could be an indication that either the latent heat fluxes were being overestimated, or that the hypothetical calculation of ET_o by the Penman–Monteith method, which is required to determine ET_c, was underestimated. Conversely, the ratio of cumulative ET_c/ET_a of the winter crops was ~1.5. This indicated that ET_c determined as a function of crop coefficients and reference evapotranspiration was overestimated. The K_c values used to estimate ET_c were originally developed through the measurement of ET_a using a weighing lysimeter. In this study, ET_a was estimated using EC systems which are able to provide a direct measure of LE, therefore, the K_c values used here may not be suitable for this particular analysis. Cumulative totals of ET_o were greater than the cumulative totals of ET_a estimated for all three

Table 6 Monthly reference, potential evapotranspiration (ET_o and ET_c; mm) and rainfall (P; mm) of maize grown in the CIA in 1998/99 and 2010/11 (adapted from Edraki et al. 2003)

Month	1998/99			2010/11		
	ET_o	ET_c	P	ET_o	ET_c	P
November	215.2	107.6	48.0	273.0	73.0	113.5
December	306.9	214.8	16.0	280.4	110.0	24.4
January	319.3	271.4	15.0	264.0	126.1	56.1
February	243.0	206.6	2.0	222.9	104.0	203.5

Table 7 Monthly reference, potential evapotranspiration (ET_o and ET_c; mm) and rainfall (P; mm) of wheat grown in the CIA in 1999 and 2011 (adapted from Edraki et al. 2003)

Month	1999			2011		
	ET_o	ET_c	P	ET_o	ET_c	P
June	30.0	18.0	51.0	93.3	56.0	14.2
July	36.9	33.2	8.0	92.7	83.4	29.0
August	62.5	68.8	45.0	90.6	95.2	62.0
September	103.8	114.2	24.0	119.8	125.7	34.3
October	155.6	124.5	42.0	129.4	103.5	18.52
November	209.2	104.6	38.0	154.3	77.1	38.6

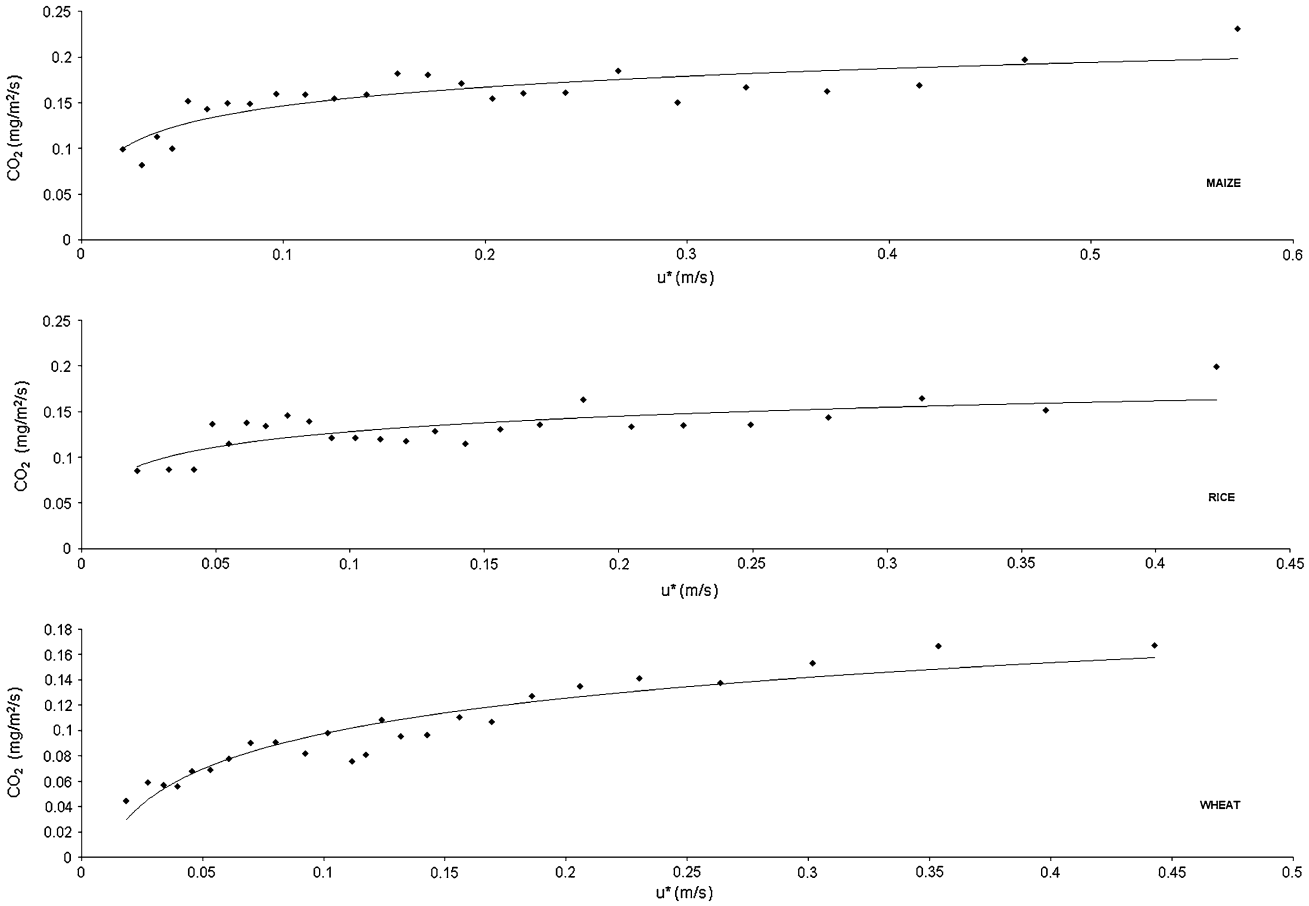

Fig. 6 *Scatter plots* of CO_2 flux versus friction velocity (u^*)

cropping systems. However, there were periods during the summer growing season when daily rates of ET_a exceeded daily rates of ET_o (data not shown). Advection may have enhanced evaporative processes during these periods, increasing evaporative demand (Alfieri et al. 2012; Alberto et al. 2011). Advection was minimal during the winter growing season because of greater levels of atmospheric stability.

Partitioning of carbon dioxide fluxes

Firstly, a friction velocity (u^*) threshold for each dataset was set to ensure turbulence intensity, whereby any data not meeting the criterion was deemed unreliable and removed from the dataset. The percentage of the 30 min averaged night-time CO_2 flux data that was subsequently selected for further analysis of maize, rice and wheat was 32.3, 16.5 and 3.0 %, respectively. The relationship between u^* and CO_2 flux is presented in Fig. 6. As mentioned the u^* threshold is located at the point where fluxes begin to decrease as u^* decreases, therefore, the u^* thresholds for rice, maize and wheat were arbitrarily identified to be 0.15, 0.17 and 0.33 m/s, respectively. The empirical exponential models required to partition CO_2 fluxes were then determined by fitting an exponential function to remaining night-time CO_2 fluxes plotted against corresponding night-time soil (T_s). Previous studies of CO_2 fluxes of rice crops reveal that it is necessary to separate flooded periods from drained periods, because CO_2 transport from the soil surface to the atmosphere is diffused during periods of permanent irrigation water application (e.g. Saito et al. 2005). However, in this study it was difficult to establish a meaningful relationship between CO_2 flux and T_s during drained conditions given the small sample set of data representative this period ($n = 5$).

The resulting empirical models and corresponding coefficients of determination (r^2) for each flux tower location are:

$$\mathrm{CO_2\ flux_{maize}} = 0.047 \exp(0.058\, T_s)\ \mathrm{mg/m^2/s};\ r^2 = 0.14$$

$$\mathrm{CO_2\ flux_{rice}} = 0.0013\exp(0.23 T_s)\ \mathrm{mg/m^2/s};\ r^2 = 0.14$$

$$\mathrm{CO_2\ flux_{wheat}} = 0.050\exp(0.040\, T_s)\ \mathrm{mg/m^2/s};\ r^2 = 0.53$$

Based on these results, the empirical models developed to determine the relationship between carbon dioxide flux

and soil temperature represent a marginal fit of the data, as emphasised by the low values of r^2. This is not uncommon in EC studies where the r^2 is often reported to be less than 0.2 (Baldocchi 2003). In this study, the relationship between carbon flux and T_s of all cropping systems was weak to moderate ($r^2 = 0.14$–0.53). Therefore, it is likely that the computed values of *Re* and GPP contain considerable error. This is not unexpected, given the multiple number of processes not included in standard respiration models that may influence CO_2 flux, e.g. the physical displacement of CO_2 following a rainfall event or the biological activity of both aboveground and belowground autotrophic biomass (Scott et al. 2006).

Cumulative total of net ecosystem exchange, gross primary productivity and total ecosystem respiration

Cumulative totals of partitioned CO_2 fluxes are presented in Table 8. In this case, a negative value of NEE represents a flux of CO_2 from the atmosphere (i.e. carbon uptake). Overall, all three crops acted as a net carbon sink, as indicated by the negative cumulative totals of NEE. The magnitude of atmospheric carbon uptake or release of a plant is partly influenced by the nature of the photosynthetic pathway. As a C4 plant, maize has a greater photosynthetic capacity compared to its C3 counterparts such as rice and wheat (Suyker et al. 2005). As such, the maize crop exhibited the greatest capacity for net carbon capture (NEE = −1,327 g C/m^2) over the observation period, whereas the cumulative total of NEE of the rice crop was −836 g C/m^2. For the wheat crop, the cumulative total of NEE was −388 g C/m^2, almost half that of its C3 summer counterpart, rice. The affinity for carbon capture was also reflected in the maximum average daily rate of NEE which peaked at −21.3 g C/m^2/day for maize and −8.7 g C/m^2/day for wheat (data not shown). This suggested that the lower temperatures and decreased net radiation experienced during the winter months had a direct effect on net carbon uptake. Whilst all three cropping systems acted as a carbon sink for the majority of the growing season, positive values of NEE (i.e. carbon release) were experienced at the beginning of the growing season for rice and wheat, thus becoming a net carbon source during this period (data not shown). This is due to the relatively small amount of photosynthetic material available for carbon assimilation, particularly at the beginning of the growing season. Because of this, respiration rates of CO_2 (Re) directly from the soil surface to the atmosphere account for the majority of the flux, especially at night.

The total amount of carbon fixed as biomass through photosynthesis (represented as GPP) of the two summer crops was greater than the winter wheat crop and can be attributed to the greater amount of photosynthetic activity as a result of increased solar radiation and mean air temperatures during the summer months. Overall, maize exhibited the greatest affinity for carbon assimilation (GPP = 1,952 g C/m^2) and was to be expected, considering maize is a C4 plant, therefore having a greater capacity for carbon capture. The cumulative totals of GPP of the rice and wheat crop were 1,514 and 1,367 g C/m^2, respectively. This is also reflected in the maximum average daily rates of GPP, which was 25.7 g C/m^2/day for maize compared to 18.2 g C/m^2/day for the rice crop. The maximum daily GPP rate for the wheat crop was only 13.1 g C/m^2/day. All three cropping systems exhibited similar temporal changes in GPP, whereby the rate of increase in GPP was slow during the early stages of vegetative growth and increased rapidly during the adult vegetative and reproductive phases (data not shown). Once physiological maturity had been reached, GPP began to decline; this was directly related to the decreased photosynthetic activity that occurred as a result of decreasing chlorophyll content due to leaf senescence (Steduto et al. 2007; Suyker and Verma 2010; Rossini et al. 2012).

Table 8 Cumulative totals of partitioned CO_2 fluxes (g C/m^2)

Crop	NEE	Re	GPP
Maize	−1,327	625	1,952
Rice	−826	629	1,514
Wheat	−388	1,367	979

The amount of carbon dioxide lost to the atmosphere (represented by Re) was least for the maize crop which had a cumulative total 625 g C/m^2 and accounted for 32.0 % of the carbon budget. The cumulative total Re of the rice crop was 689 g C/m^2 that represented 45.5 % of the carbon budget. For the winter wheat crop, the cumulative season total of Re was 979 g C/m^2 which represented 71.6 % of the carbon budget. Decreased respiration rates of maize can be partially attributed to the fact that photorespiration (i.e. respiration during the photosynthetic process) is greatly reduced in C4 plants by inhibiting the enzymatic oxygenation activity (Kennedy 1976; Lara and Andreo 2011). Increased respiration of the winter wheat crop can be partly attributed to land preparation prior to sowing. For example, the crop was sown directly into the stubble of the previous maize crop which meant that there was a larger volume of organic material available for decomposition which led to greater proportions of Re throughout the growing season.

Summary and conclusions

There are very few studies that have reported an integrated quantitative assessment of energy, water vapour and carbon

dioxide fluxes of Australian irrigated broad-acre agricultural cropping systems. For the first time, this study presents a detailed analysis of the estimation and seasonal distribution of energy, water vapour and carbon dioxide fluxes of three of the major irrigated crops grown in inland Australia; maize, rice and wheat, using EC methodologies.

The first objective of the study presented in this paper was to quantify and compare atmospheric fluxes of water, carbon and energy of three commonly irrigated broad-acre crops (maize, rice and wheat) within a semi-arid Australian irrigated context over the summer and winter growing seasons. There was a distinct seasonal difference in the flux magnitudes of water, carbon and energy. The magnitude of latent heat exchange of the two summer crops was 1.5–2.0 times greater than that of the winter wheat crop. In addition, irrigation management practices affected the distribution of turbulent fluxes, as demonstrated by the energy budget for rice which was predominately driven by latent heat exchange. The seasonal budget of evapotranspiration of rice was 25 % greater than that of maize.

The second objective of this study was to determine whether irrigated agro-ecosystems in Australian semi-arid climate zones are net sources or sinks of carbon dioxide. Overall, it was found that all three cropping systems acted as a net carbon sink over each growing season, although small pulses of CO_2 into the atmosphere were observed in the early vegetative stages of growth and at times during leaf senescence. Maize exhibited the greatest affinity for carbon assimilation (i.e. the total amount of carbon fixed as biomass; GPP). The cumulative seasonal total GPP of maize was $\sim$20–40 % greater than for rice and wheat cropping systems. This is to be expected, given that maize has a C4 photosynthetic pathway. As a crop species, maize exhibited the greatest seasonal net carbon capture (NEE), followed by rice. Like GPP, this can be attributed to the greater affinity of the C4 photosynthetic pathway of maize and the reduced loss of carbon dioxide through greater stomatal control. As a crop, wheat exhibited the least net carbon capture. This can be attributed in part to the smaller amount of biomass production relative to the summer crops as reflected by the smaller grain yield.

The results of this study serve to fill the knowledge gap with respect to the mass and energy exchange of broad-acre cropping systems in Australian dryland irrigation areas. By doing this we can begin to understand the influence of irrigated agriculture on the daily fluxes of carbon dioxide, water vapour and energy and the way in which it affects the local and regional climate. However, it is acknowledged that studies of atmospheric-land surface interactions for single growing seasons or years are insufficient when trying to understand the long-term processes that drive agro-ecosystem functions. Therefore, it is necessary to conduct long-term experiments using EC technologies to compare the interannual variability of different cropping systems and the influence of varying meteorological conditions and Australian irrigated agricultural management practices. Furthermore, point-based EC methods can only provide information regarding the atmospheric-land surface exchange within a finite area. To quantify the mass and energy balance at greater spatial scales, upscaling EC data via numerical modelling in conjunction with remote sensing data from satellites designed specifically to measure atmospheric water and carbon dioxide (e.g. GOSAT) could assist in the closing of regional and global water and carbon budgets. Information derived from these studies can then be used to inform policy and shape current and future water-saving and climate change adaption initiatives.

Acknowledgments Financial support for this study was provided via the Coleambally Water Smart Australia project, commissioned by the National Water Commission of Australia. The authors would like to thank Mohsin Hafeez for the opportunity to explore this study, Rolf Faux for his assistance with instrument deployment and data collection; James Cleverly, Peter Isaac and Ray Leuning for their time and instruction of data processing techniques and quality control procedures; the landholders for unlimited access to their properties; other staff and students of the former International Centre of Water for Food Security who collated ancillary data; and Michael Wilson and Austin Evans of CICL who provided access to crop water use information for the CIA.

References

Alberto MCR, Wassmann R, Hirano T, Miyata A, Kumar A, Padre A, Amante M (2009) CO2/heat fluxes in rice fields: comparative assessment of flooded and non-flooded fields in the Philippines. Agric For Meteorol 149(10):1737–1750. doi:10.1016/j.agrformet.2009.06.003

Alberto MCR, Wassmann R, Hirano T, Miyata A, Hatano R, Kumar A, Padre A, Amante M (2011) Comparisons of energy balance and evapotranspiration between flooded and aerobic rice fields in the Philippines. Agric Water Manag 98(9):1417–1430. doi:10.1016/j.agwat.2011.04.011

Alfieri JG, Kustas WP, Prueger JH, Hipps LE, Evett SR, Basara JB, Neale CMU, French AN, Colaizzi P, Agam N, Cosh MH, Chavez JL, Howell TA (2012) On the discrepancy between eddy covariance and lysimetry-based surface flux measurements under strongly advective conditions. Ad Water Resour 50:62–78. doi:10.1016/j.advwatres.2012.07.008

Allen RG, Pereira LS, Raes D, Smith M (1988) Crop evapotranspiration—Guidelines for computing crop water requirements. FAO Irrigation and drainage paper, vol 300

Australian Bureau of Statistics (2012a) Gross value of irrigated agricultural production, 2010–2011. Canberra

Australian Bureau of Statistics (2012b) Value of agricultural commodities produced, Australia, 2010–2011. Canberra

Australian Bureau of Statistics (2012c) Water account Australia: 2010–2011. Canberra

Baldocchi D (2003) Assessing the eddy covariance technique for evaluating carbon dioxide exchange rates of ecosystems: past, present and future. Global Change Biol 9(4):479–492. doi:10.1046/j.1365-2486.2003.00629.x

Baldocchi D, Falge E, Gu LH, Olson R, Hollinger D, Running S, Anthoni P, Bernhofer C, Davis K, Evans R, Fuentes J, Goldstein

A, Katul G, Law B, Lee XH, Malhi Y, Meyers T, Munger W, Oechel W, KTP U, Pilegaard K, Schmid HP, Valentini R, Verma S, Vesala T, Wilson K, Wofsy S (2001) FLUXNET: a new tool to study the temporal and spatial variability of ecosystem-scale carbon dioxide, water vapor, and energy flux densities. Bull Am Meteorol Soc 82(11):2415–2434

Brutsaert W (1982) Evaporation into the atmosphere: theory, history, and applications, Environmental Fluid Mechanics, vol 1. D. Reidel Publishing Co., Dordrecht

Burba GG (2013) Eddy covariance method for scientific, industrial, agricultural, and regulatory applications, LI-COR biosciences. Lincoln, Nebraksa

Burba GG, Anderson DJ (2010) A brief practical guide to Eddy covariance flux measurements: principles and workflow examples for scientific and industrial applications LI-COR biosciences. Lincoln, USA

Bureau of Meteorology (2005) Australian climate zones—major classification groups. Commonwealth of Australia. http://www.bom.gov.au/climate/environ/other/kpn_group.shtml. Accessed 9 Jul 2010

Bureau of Meteorology (2012) Climate statistics for Australian locations—Griffith Airport AWS 075041. http://www.bom.gov.au/climate/averages/tables/cw_075041.shtml. Accessed 18 Apr 2012

Coleambally Irrigation Cooperative Ltd (2010) Annual Compliance Report 2010

Coleambally Irrigation Cooperative Ltd (2011) Annual Compliance Report 2011

De Datta SK (1987) Principles and practices of rice production. Krieger, Malabar

Department of Climate Change and Energy Efficiency (2011) Australian National Greenhouse Accounts: National Inventory Report 2009. vol 2

Domingo F, Serrano-Ortiz P, Were A, Villagarcía L, García M, Ramírez DA, Kowalski AS, Moro MJ, Rey A, Oyonarte C (2011) Carbon and water exchange in semiarid ecosystems in SE Spain. J Arid Environ 75(12):1271–1281. doi:10.1016/j.jaridenv.2011.06.018

Edraki M, Smith D, Humphreys E, Khan S, O'Connell N, Xevi E (2003) Validation of the SWAGMAN Farm and SWAGMAN Destiny models. Technical Report. CSIRO Land and Water, Griffith, NSW, Australia

Evans GN (1971) Evaporation from rice at griffith, New South Wales. Agric Meteorol 8:117–127. doi:10.1016/0002-1571(71)90101-4

Evrendilek F, Karakaya N, Aslan G, Ertekin C (2011) Using Eddy covariance sensors to quantify carbon metabolism of Peatlands: a case study in Turkey. Sensors 11(1):522–538

Falge E, Baldocchi D, Olson R, Anthoni P, Aubinet M, Bernhofer C, Burba G, Ceulemans R, Clement R, Dolman H, Granier A, Gross P, Grünwald T, Hollinger D, Jensen N-O, Katul G, Keronen P, Kowalski A, Lai CT, Law BE, Meyers T, Moncrieff J, Moors E, Munger JW, Pilegaard K, Rannik Ü, Rebmann C, Suyker A, Tenhunen J, Tu K, Verma S, Vesala T, Wilson K, Wofsy S (2001) Gap filling strategies for defensible annual sums of net ecosystem exchange. Agric For Meteorol 107(1):43–69

Falge E, Baldocchi D, Tenhunen J, Aubinet M, Bakwin P, Berbigier P, Bernhofer C, Burba G, Clement R, Davis KJ, Elbers JA, Goldstein AH, Grelle A, Granier A, Guðmundsson J, Hollinger D, Kowalski AS, Katul G, Law BE, Malhi Y, Meyers T, Monson RK, Munger JW, Oechel W, Paw UKT, Pilegaard K, Rannik Ü, Rebmann C, Suyker A, Valentini R, Wilson K, Wofsy S (2002) Seasonality of ecosystem respiration and gross primary production as derived from FLUXNET measurements. Agric For Meteorol 113(1–4):53–74 10.1016/S0168-1923(02)00102-8

Foken T, Wimmer F, Mauder M, Thomas C, Liebethal C (2006) Some aspects of the energy balance closure problem. Atmos Chem Phys 6(12):4395–4402. doi:10.5194/acp-6-4395-2006

Foken T, Mauder M, Liebethal C, Wimmer F, Beyrich F, Leps J-P, Raasch S, DeBruin H, Meijninger W, Bange J (2010) Energy balance closure for the LITFASS-2003 experiment. Theor Appl Climatol 101:149–160

Foley JA, DeFries R, Asner GP, Barford C, Bonan G, Carpenter SR, Chapin FS, Coe MT, Daily GC, Gibbs HK, Helkowski JH, Holloway T, Howard EA, Kucharik CJ, Monfreda C, Patz JA, Prentice IC, Ramankutty N, Snyder PK (2005) Global consequences of land use. Science 309(5734):570–574. doi:10.1126/science.1111772

Gilmanov TG, Aires L, Barcza Z, Baron VS, Belelli L, Beringer J, Billesbach D, Bonal D, Bradford J, Ceschia E, Cook D, Corradi C, Frank A, Gianelle D, Gimeno C, Gruenwald T, Guo H, Hanan N, Haszpra L, Heilman J, Jacobs A, Jones MB, Johnson DA, Kiely G, Li S, Magliulo V, Moors E, Nagy Z, Nasyrov M, Owensby C, Pinter K, Pio C, Reichstein M, Sanz MJ, Scott R, Soussana JF, Stoy PC, Svejcar T, Tuba Z, Zhou G (2010) Productivity, respiration, and light-response parameters of world grassland and agroecosystems derived from flux-tower measurements. Rangel Ecol Manag 63(1):16–39. doi:10.2111/rem-d-09-00072.1

Goulden ML, McMillan AMS, Winston GC, Rocha AV, Manies KL, Harden JW, Bond-Lamberty BP (2011) Patterns of NPP, GPP, respiration, and NEP during boreal forest succession. Global Change Biol 17(2):855–871. doi:10.1111/j.1365-2486.2010.02274.x

Hatala JA, Detto M, Sonnentag O, Deverel SJ, Verfaillie J, Baldocchi DD (2012) Greenhouse gas (CO2, CH4, H2O) fluxes from drained and flooded agricultural peatlands in the Sacramento-San Joaquin Delta. Agric Ecosyst Environ 150:1–18. doi:10.1016/j.agee.2012.01.009

Humphreys E, Meyer W, Prathapar S, Smith D (1994) Estimation of evapotranspiration from rice in southern New South Wales: a review. Aust J Exp Agric 34(7):1069–1078. Doi:10.1071/EA9941069

Inagaki A, Letzel MO, Raasch S, Kanda M (2006) Impact of surface heterogeneity on energy imbalance: a study using LES. J Meteorol Soc Japan Ser II 84(1):187–198

Intergovernmental Panel on Climate Change (2007) Climate Change 2007: Synthesis Report. Contribution of Working Groups I, II and III to the Fourth Assessment Report of the Intergovernmental Panel on Climate Change. Geneva, Switzerland

Isaac P, Cleverly J (2011) OzFlux QC. 1.5 edn. CSIRO, Canberra, Australia

Jackson TM, Khan S, Hafeez M (2010) A comparative analysis of water application and energy consumption at the irrigated field level. Agric Water Manag 97(10):1477–1485. doi:10.1016/j.agwat.2010.04.013

Jans WWP, Jacobs CMJ, Kruijt B, Elbers JA, Barendse S, Moors EJ (2010) Carbon exchange of a maize (*Zea mays* L.) crop: influence of phenology. Agric Ecosyst Environ 139(3):316–324. doi:10.1016/j.agee.2010.06.008

Kalfas JL, Xiao X, Vanegas DX, Verma SB, Suyker AE (2011) Modelling gross primary production of irrigated and rain-fed maize using MODIS imagery and CO2 flux tower data. Agric For Meteorol 151(12):1514–1528

Kanniah KD, Beringer J, Hutley LB (2011) Environmental controls on the spatial variability of savanna productivity in the Northern Territory, Australia. Agric For Meteorol 151(11):1429–1439. doi:10.1016/j.agrformet.2011.06.009

Kennedy RA (1976) Photosynthesis and photorespiration in C3 and C4 plant-tissue cultures—significance of Kranz anatomy to operation of C4 pathway. Plant Physiol 57(5):53

Khan S, Hanjra MA (2009) Footprints of water and energy inputs in food production—global perspectives. Food Policy 34(2):130–140

Kilinc M, Beringer J, Hutley LB, Haverd V, Tapper N (2012) An analysis of the surface energy budget above the world's tallest angiosperm forest. Agric For Meteorol 166–167(0):23–31. Doi:10.1016/j.agrformet.2012.05.014

Kirschbaum MUF, Saggar S, Tate KR, Thakur KP, Giltrap DL (2013) Quantifying the climate-change consequences of shifting land use between forest and agriculture. Sci Total Environ 465(0):314–324. Doi:10.1016/j.scitotenv.2013.01.026

Lara MV, Andreo CS (2011) C4 plants adaptation to high levels of CO2 and to drought environments. In: Shanker A, Venkateswarlu B (eds) Abiotic stress in plants—mechanisms and adaptations. InTech. doi:10.5772/24936

Lee X, Law B, Massman W (2004) Handbook of micrometeorology: a guide for surface flux measurement and analysis. Springer, Netherlands

Leuning R (2004) Measurements of trace gas fluxes in the atmosphere using eddy covariance: WPL corrections revisited. In: Lee X, Massman WJ, Law B (eds) Handbook of micrometeorology: a guide for surface flux measurement and analysis. Springer, Netherlands, pp 119–132

Leuning R, Cleugh HA, Zegelin SJ, Hughes D (2005) Carbon and water fluxes over a temperate eucalyptus forest and a tropical wet/dry savanna in Australia: measurements and comparison with MODIS remote sensing estimates. Agric For Meteorol 129(3–4):151–173

Lloyd J, Taylor JA (1994) On the temperature dependence of soil respiration. Funct Ecol 8(3):315–323

Loescher HW, Law BE, Mahrt L, Hollinger DY, Campbell J, Wofsy SC (2006) Uncertainties in, and interpretation of, carbon flux estimates using the eddy covariance technique. J Geophys Res Atmos 111(D21). doi:10.1029/2005jd006932

Long KD (2008) Methane fluxes from a northern peatland: mechanisms controlling diurnal and seasonal variation and the magnitude of aerobic methanogensis. University of Lethbridge, Lethbridge

Massman WJ (2000) A simple method for estimating frequency response corrections for eddy covariance systems. Agric For Meteorol 104(3):185–198

Massman WJ (2001) Reply to comment by Rannik on "A simple method for estimating frequency response corrections for eddy covariance system". Agric For Meteorol 107(3):247–251. doi:10.1016/S0168-1923(00)00237-9

Massman WJ, Clement R (2004) Uncertainty in eddy covariance flux estimates resulting from spectral attenuation. In: Lee X, Massman W, Law B (eds) Handbook of micrometeorology: a guide for surface flux measurement and analysis. Springer, Netherlands, pp 67–99

McVicar T, Van Niel T (2012) Coleambally: an agricultural time series site. CSIRO. http://www.eoc.csiro.au/hswww/oz_pi/colly_site/key.htm. Accessed 26 Jul 2012

Meyer WS, Smith DJ, Shell G (1999) Estimating reference evaporation and crop evapotranspiration from weather data and crop coefficients: An addendum to AWRAC Research Project 84/162—Quantifying components of the water balance under irrigated crops. Technical Report. CSIRO Land and Water, Griffith, NSW, Australia

Moffat AM, Papale D, Reichstein M, Hollinger DY, Richardson AD, Barr AG, Beckstein C, Braswell BH, Churkina G, Desai AR, Falge E, Gove JH, Heimann M, Hui DF, Jarvis AJ, Kattge J, Noormets A, Stauch VJ (2007) Comprehensive comparison of gap-filling techniques for eddy covariance net carbon fluxes. Agric For Meteorol 147(3–4):209–232. doi:10.1016/j.agrformet.2007.08.011

Moncrieff J, Clement R, Finnigan J, Meyers T (2004) Averaging, Detrending, and Filtering of Eddy Covariance Time Series. In: Lee X, Massman W, Law B (eds) Handbook of Micrometeorology, vol 29. Atmospheric and Oceanographic Sciences Library. Springer, Netherlands, pp 7–31. doi:10.1007/1-4020-2265-4_2

Murrumbidgee Irrigation Ltd (2013) Rice water use in the murrumbidgee irrigation area. http://www.mirrigation.com.au/Customers/Rice-Water-Use-Targets. Accessed 25 Mar 2013

Neftel A, Spirig C, Ammann C (2008) Application and test of a simple tool for operational footprint evaluations. Environ Pollut 152(3):644–652

Oncley SP, Foken T, Vogt R, Kohsiek W, DeBruin HAR, Bernhofer C, Christen A, van Gorsel E, Grantz D, Feigenwinter C, Lehner I, Liebethal C, Liu H, Mauder M, Pitacco A, Ribeiro L, Weidinger T (2007) The energy balance experiment EBEX-2000. Part I: overview and energy balance. Bound Layer Meteorol 123(1):1–28

Ramankutty N, Evan AT, Monfreda C, Foley JA (2008) Farming the planet: 1. Geographic distribution of global agricultural lands in the year 2000. Global Biogeochem Cycles 22(1):GB1003. doi:10.1029/2007gb002952

Reichstein M, Falge E, Baldocchi D, Papale D, Aubinet M, Berbigier P, Bernhofer C, Buchmann N, Gilmanov T, Granier A, Grunwald T, Havrankova K, Ilvesniemi H, Janous D, Knohl A, Laurila T, Lohila A, Loustau D, Matteucci G, Meyers T, Miglietta F, Ourcival J-M, Pumpanen J, Rambal S, Rotenberg E, Sanz M, Tenhunen J, Seufert G, Vaccari F, Vesala T, Yakir D, Valentini R (2005) On the separation of net ecosystem exchange into assimilation and ecosystem respiration: review and improved algorithm. Global Change Biol 11(9):1424–1439 citeulike-article-id:299299

Rossini M, Cogliati S, Meroni M, Migliavacca M, Galvagno M, Busetto L, Cremonese E, Julitta T, Siniscalco C, Morra di Cella U, Colombo R (2012) Remote sensing-based estimation of gross primary production in a subalpine grassland. Biogeosciences 9(7):2565–2584. doi:10.5194/bg-9-2565-2012

Saito M, Miyata A, Nagai H, Yamada T (2005) Seasonal variation of carbon dioxide exchange in rice paddy field in Japan. Agric For Meteorol 135(1–4):93–109. doi:10.1016/j.agrformet.2005.10.007

Scott RL, Huxman TE, Cable WL, Emmerich WE (2006) Partitioning of evapotranspiration and its relation to carbon dioxide exchange in a Chihuahuan Desert shrubland. Hydrol Process 20(15):3227–3243. doi:10.1002/hyp.6329

Scott RL, Serrano-Ortiz P, Domingo F, Hamerlynck EP, Kowalski AS (2012) Commonalities of carbon dioxide exchange in semiarid regions with monsoon and Mediterranean climates. J Arid Environ 84:71–79. doi:10.1016/j.jaridenv.2012.03.017

Spiertz H (2012) Avenues to meet food security. The role of agronomy on solving complexity in food production and resource use. Eur J Agron 43:1–8. doi:10.1016/j.eja.2012.04.004

Steduto P, Hsiao TC, Fereres E (2007) On the conservative behavior of biomass water productivity. Irrig Sci 25(3):189–207. doi:10.1007/s00271-007-0064-1

Stoy PC, Mauder M, Foken T, Marcolla B, Boegh E, Ibrom A, Arain MA, Arneth A, Aurela M, Bernhofer C, Cescatti A, Dellwik E, Duce P, Gianelle D, van Gorsel E, Kiely G, Knohl A, Margolis H, McCaughey H, Merbold L, Montagnani L, Papale D, Reichstein M, Saunders M, Serrano-Ortiz P, Sottocornola M, Spano D, Vaccari F, Varlagin A (2013) A data-driven analysis of energy balance closure across FLUXNET research sites: The role of landscape scale heterogeneity. Agric For Meteorol 171–172(0):137–152. Doi:10.1016/j.agrformet.2012.11.004

Suyker AE, Verma SB (2010) Coupling of carbon dioxide and water vapor exchanges of irrigated and rainfed maize-soybean cropping systems and water productivity. Agric For Meteorol 150(4):553–563

Suyker AE, Verma SB, Burba GG, Arkebauer TJ (2005) Gross primary production and ecosystem respiration of irrigated maize

and irrigated soybean during a growing season. Agric For Meteorol 131(3–4):180–190. doi:10.1016/j.agrformet.2005.05.007

The World Bank (2007) World Development Report 2008: Agriculture for Development. The World Bank, Washington, DC

Tsai J-L, Tsuang B-J, Lu P-S, Yao M-H, Yuan S (2007) Surface energy components and land characteristics of a rice paddy, vol 46. vol 11. American Meteorological Society, Boston, MA, USA

Webb EK, Pearman GI, Leuning R (1980) Correction of flux measurements for density effects due to heat and water vapour transfer. Quart J Roy Meteorol Soc 106(447):85–100. doi:10.1002/qj.49710644707

Wilson KB, Baldocchi DD, Aubinet M, Berbigier P, Bernhofer C, Dolman H, Falge E, Field C, Goldstein A, Granier A, Grelle A, Halldor T, Hollinger D, Katul G, Law BE, Lindroth A, Meyers T, Moncrieff J, Monson R, Oechel W, Tenhunen J, Valentini R, Verma S, Vesala T, Wofsy S (2002) Energy partitioning between latent and sensible heat flux during the warm season at FLUXNET sites. Water Resour Res 38(12):30-1–30-11. doi:10.1029/2001wr000989

Wohlfahrt G, Bahn M, Haslwanter A, Newesely C, Cernusca A (2005) Estimation of daytime ecosystem respiration to determine gross primary production of a mountain meadow. Agric For Meteorol 130(1–2):13–25. doi:10.1016/j.agrformet.2005.02.001

Yu Q, Wu W, Yang P, Li Z, Xiong W, Tang H (2012) Proposing an interdisciplinary and cross-scale framework for global change and food security researches. Agric Ecosyst Environ 156:57–71. doi:10.1016/j.agee.2012.04.026

Zhang Z, Jiang H, Liu J, Weimin J, Xiuying Z (2013) Effect of heterogeneous atmospheric CO2 onsimulated global carbon budget. Glob Planet Chang. doi:10.1016/j.gloplacha.2012.12.002